

Hydraulic properties of household waste and implications for landfills

W. Powrie, MA, MSc, PhD, CEng, FICE and R. P. Beaven, BA, MSc, FGS

■ A series of tests has been carried out on crude unprocessed household waste in a large purpose-built compression cell, to investigate the variations in density, drainable porosity and hydraulic conductivity with vertical stress. An increase in the particle density of the waste with increasing stress was identified; this may mean that the applicability of some standard soil mechanics theories to household waste may need to be reviewed. The results of the tests are described and discussed, with reference to their implications for the flow and control of leachate in landfills. The hydrogeological limitations on vertical flushing rates in landfills operated as flushing bioreactors are considered and the operation and performance of leachate extraction wells investigated by means of simple analytical models.

Keywords: groundwater; landfill; research & development

Notation

A	cross-sectional area
B	parameter defined in text
D	depth of landfill
F	side force due to friction
FC	field capacity
H	initial head in well analysis
h	head
h_w	head in well
i	hydraulic gradient
k	hydraulic conductivity
m_s	mass of dry solids
n	porosity
n_e	drainable porosity
P	applied pressure in compression cell test
q	volumetric flow rate
r_o	radius of influence of a pumped well
r_w	radius of pumped well
u	pore water pressure
V	volume
V_s	volume of dry solids
V_v	volume of voids
v	specific volume
WC_{dry}	water content by dry mass (m_{water}/m_{solids})
WC_{wet}	water content by wet (total) mass (m_{water}/m_{total})
WC_{vol}	volumetric water content by total volume (V_{water}/V_{total})

w	water content by dry mass (m_{water}/m_{solids})
z	depth ordinate
α	parameter defining thickness of overburden layer
γ	unit weight
δ	prefix denoting elemental increment
δ	interface friction angle between steel and waste
ρ	bulk density
ρ_{dry}	dry bulk density
ρ_{FC}	bulk density at field capacity
ρ_s	particle density
ρ_{sat}	saturated bulk density
ρ_{wet}	wet bulk density
σ_h	horizontal stress
σ_v	vertical stress
ϕ'	angle of shearing resistance (internal angle of friction)
'	denotes effective stress or effective stress parameter

Introduction

In recent years, the driving principle of landfill management in both Europe and the USA has been to prevent saturation of the waste to reduce the potential for leachate leakage into the surrounding ground. This has resulted in very slow rates of waste degradation and leaching. Consequently, removal of the pollution load from the waste occurs very slowly, so that landfills retain the potential to pollute over a time-scale measured in hundreds of years.¹ There is no doubt that waste degradation could be accelerated by circulating fluids through the waste in a controlled manner, and by operating landfills as engineered flushing bioreactors. This concept, which is espoused by a Department of the Environment (DOE) waste management paper,² offers significant potential environmental benefits and is consistent with the aims of the sustainable waste management policy.³ However, its successful implementation requires an understanding of the factors governing the hydraulic properties of wastes, and their impact on the flow of fluids within the waste mass.

2. Even in a conventional landfill, any attempt to control leachate levels (e.g. by pumping from vertical wells) requires an understanding of the hydraulic properties of the waste and how these may change with increasing effective stress.

3. In this paper, an experimental investiga-

*Proc. Instn
Civ. Engrs
Geotech. Engng,
1999, 137, Oct.,
235-247*

Paper 11854

*Written discussion
closes 31 March 2000*

*Manuscript received
26 October 1998;
revised manuscript
accepted 19 May
1999*

*W. Powrie, Professor
of Geotechnical
Engineering,
Department of Civil
and Environmental
Engineering,
University of
Southampton*

*R. P. Beaven, Senior
Research Fellow,
Department of Civil
and Environmental
Engineering,
University of
Southampton (also of
Richard Beaven
Associates, Maldon)*

tion into the influence of vertical stress on waste density, porosity and hydraulic conductivity of household waste is described. The implications of the results for the design and operation of a landfill as a simple flushing bioreactor and for the effectiveness of conventional leachate extraction wells are discussed.

Definition of terms

4. In general, fresh refuse will contain some water but will not be saturated. The water content (w or WC_{dry}) of the refuse as deposited is referred to as the *original water content*, and is defined and determined in the conventional soil mechanics way as the ratio of the mass of water to the mass of dry solids. Water contents are also sometimes expressed in terms of the ratio of the mass of water to the total mass of water and solids (WC_{wet}) or as the ratio of the volume of water to the total volume of air, solids and water (WC_{vol}).

5. After landfilling, the water content of the waste may increase through the absorption of water by components such as paper, cardboard and textiles. Beyond a certain limit, known as the *total absorptive capacity* of the waste, the addition of any further water leads to the production of an equivalent volume of free-draining pore fluid, which will tend to move downward under the influence of gravity towards a 'water' table below which (in the absence of landfill gas production) the waste is substantially saturated.

6. Refuse is referred to as being at *field capacity* when its total absorptive capacity has been fully utilized and conditions of free downward drainage established. In the tests described in this paper, the total absorptive capacity and the field capacity were determined by flooding the refuse from the bottom of the sample, and then allowing it to drain. This procedure also enables the *drainable porosity* of the refuse, n_e (defined as the volume of drainable voids per unit total volume), at field capacity to be determined.

7. The *bulk density* of the refuse, ρ , is important, because it is used to calculate vertical stresses at depth. As with soils, the *dry density*, ρ_{dry} , is sometimes used as an indication of the degree of compaction of the refuse. ρ_{dry} is the density that the refuse would have at the same total (gas + liquid) void ratio but zero water content. It is well-known that

$$\rho_{dry} = \frac{\rho}{(1 + w)} \tag{1}$$

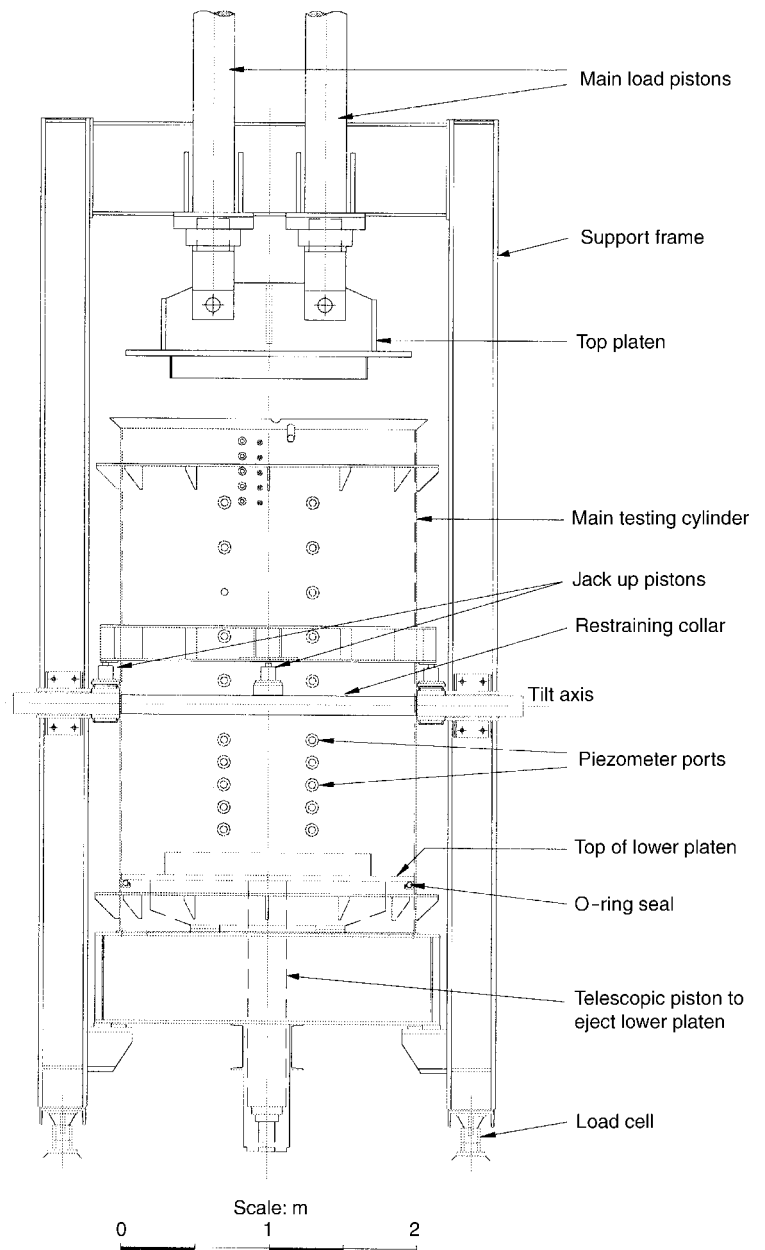
where w (or WC_{dry}) is the actual water content.⁴

The Pitsea compression cell

8. The tests were carried out in a large purpose-built compression cell, located at Cleanaway Ltd's Pitsea landfill site in Essex, England. The cell consists of a steel cylinder,

2 m in diameter and 3 m high, into which refuse is placed for testing (Fig. 1). The cylinder is suspended vertically within a steel support frame. The feet of the support frame are mounted on load cells, enabling the weight of the contents of the cell to be monitored continuously. The base of the cylinder is sealed by a 2 m diameter platen seated on an O-ring. Refuse in the cylinder is compressed by an upper platen, just under 2 m in diameter (leaving an annular clearance gap of 2 mm), which can be moved vertically up or down inside the testing cylinder. The upper platen is connected to, and moved by, two 200 mm diameter hydraulically operated pistons. At the start of a test the upper platen is lowered onto the refuse: a constant vertical load can then be applied by means of the hydraulic pistons. The

Fig. 1. The Pitsea compression cell



maximum vertical load is 1900 kN, giving a vertical stress of 600 kPa distributed uniformly over the plan area of the sample.

9. During a test, water can be introduced to the bottom of the sample from two 450 l water header tanks mounted on a scaffold tower up to 3 m above the top of the testing cylinder. Pipes connect the tank outlets to twelve evenly spaced 25 mm diameter ports on the lower platen. Water flows up through the sample and out of the upper platen through twelve similar ports, and also through the 2 mm annular clearance gap between the outer edge of the platen and the inner surface of the testing cylinder. In-line electromagnetic flow meters are used to record the total volumes and flow rates of water entering and leaving the sample.

10. Following placement of the refuse, 18 piezometers were installed horizontally through ports in the side of the cylinder, located at vertical spacings of between 150 mm and 400 mm.

11. The height:diameter ratio of the Pitsea compression cell is 3:2, which is six times that of a conventional oedometer. There was therefore some concern that, in the Pitsea cell, there may be a significant reduction in vertical stress with depth within the sample due to sidewall friction, and three different approaches were adopted in an attempt to quantify this.

12. First, the theoretical reduction in stress due to sidewall friction was estimated by considering the stresses and forces acting on a waste layer of thickness δz at a depth z within the compression cell (Fig. 2).

13. Assuming that the horizontal effective stress σ'_h may be related to the vertical stress σ'_v by⁵

$$\sigma'_h = (1 - \sin \phi') \sigma'_v \quad (2)$$

(where ϕ' is the internal angle of friction) and neglecting variations in the unit weight γ of the waste, the analysis presented in Fig. 2 leads to the expression⁶

$$\sigma'_v = \frac{\gamma}{B} (1 - e^{-Bz}) + P e^{-Bz} \quad (3)$$

where

$$B = \left[\frac{4(1 - \sin \phi') \tan \delta}{d} \right]$$

The full derivation is reproduced in Appendix 1.

14. Equation (3) was used to calculate the ratio of the transmitted effective stress (σ'_v) to the applied pressure (P) with depth for various values of δ and ϕ' . Jessberger and Kockel⁷ reported values of ϕ' for wastes of up to 46° , with an apparent reduction occurring as refuse ages. Very large strains (perhaps up to 50%) were generally required to mobilize the full strength of the refuse. An indication of the angle of friction between household waste and

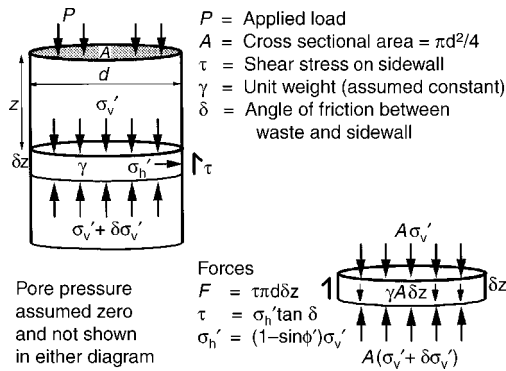


Fig. 2. Conceptual model of stresses and forces acting on waste in compression cell

the walls of the compression cell was obtained by placing approximately 1 t of loosely compacted household waste on the smooth metal back (body) of a tipper lorry. The body was slowly raised and the angle to the horizontal at which the refuse just started to move was measured. The test was repeated a number of times, giving angles of interface friction in the range 25 – 30° .

15. It is considered that the nature of the two surfaces was sufficiently similar for the angle of waste/metal friction measured in the lorry to be reasonably representative of that in the Pitsea compression cell.

16. With $\phi' = 40^\circ$ and $\delta = 25^\circ$, equation (3) indicates that approximately 75% of the applied load is transmitted to a depth of 1 m and 54% of the applied load is transmitted to a depth of 2 m. The worst case is when $\delta = \phi' = 38^\circ$ (when B is a maximum), which results in approximately 33% of the applied load being transmitted to a depth of 2 m.

17. Secondly, oil-filled vibrating wire pressure cells, 300 mm in diameter (Soil Instruments Ltd model 1.21), were installed at three depths within the compression cell to measure total vertical stresses. Two cells were installed in the waste and one cell in a basal gravel drainage layer. The cell installed in the gravel was calibrated in a 500 mm diameter laboratory oedometer, and was found to over-read the stress by approximately 17%.

18. It was not possible to calibrate directly the two cells installed in the waste. However, as these cells were installed in the same way, the degree of under- or over-read should be similar in each case. The ratio of the readings from the two cells in the waste was therefore related to the estimated vertical distance between the cells (which decreased during the experiment as the applied stress was increased and the waste compressed).

19. The variation with depth of (a) the ratio of the vertical stress transmitted to the gravel to the applied pressure and (b) the ratio of the stresses recorded in the lower and upper cells installed in the waste is shown in Fig. 3. The results of calculations using equation (3) are

also given. It may be seen that the pressure cell data are generally in reasonable agreement with equation (3) using $\phi' = 40^\circ$ and $\delta = 30^\circ$; in interpreting the test data, this relationship was used to estimate the average stress over a given depth range within the cell at a given applied load.

20. Thirdly, an attempt was made to measure the differential compression of the waste at various depths by using strings inserted through piezometer ports at different vertical heights. However, it was found that the data produced were not reliable and could not be used to estimate the effects of sidewall friction.

Experimental procedure

21. At the beginning of the test, a 145 mm thick layer of gravel was placed on the lower platen prior to refuse being loaded into the cell using a lorry-mounted hydraulic grab. An oil-filled pressure cell was installed in a pocket lined with sand within this gravel layer. A layer of refuse was placed loosely in the cell, levelled and then compressed using the upper platen to the desired initial *in situ* bulk density of approximately 0.5 Mg/m³. Further layers of refuse were loaded and compressed until the overall refuse depth was about 2.5 m. Approximately five layers were needed to fill the cell. Two further pressure cells were installed during filling at different depths within the waste. The total weight of waste in the cell was measured using the load cells mounted under the feet of the compression cell. A final layer of gravel was placed on top of the refuse.

22. Representative samples of the waste were taken throughout the filling process to produce a total subsample of mass 1.9 t, which was processed to produce a size and material classification according to the procedure described by Poll.⁸ Further subsamples of the 1.9 t of waste were taken and dried at 105°C to determine the water content. The bulk density of the refuse ρ was determined from the mass of the refuse and the volume occupied in the compression cell. The initial dry density was calculated using equation (1).

23. The upper platen was lowered onto the sample and an initial load was applied using the hydraulic system. The compression of the refuse with time was monitored by measuring the downward movement of the upper platen. Any leachate squeezed out of the refuse was collected and its volume recorded. The applied stress was maintained until compression had ceased: for practical purposes this was taken to be when the rate of change of refuse depth had fallen to less than 1% in 24 h, which normally took between two and seven days. The total vertical stresses indicated by the pressure cells installed at various depths within the refuse were also recorded.

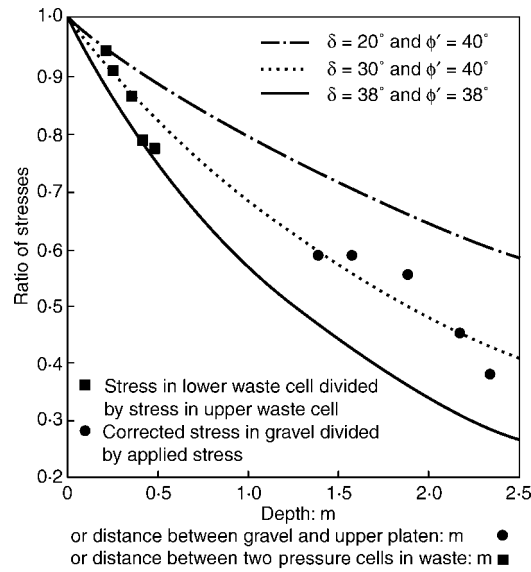


Fig. 3. Variation with depth of the vertical stress transmitted to the waste (as a proportion of the applied pressure)

24. When compression had substantially ceased, the drainable porosity of the waste was measured at constant vertical load. The waste was saturated by allowing water to flow into the sample through the lower platen. After the refuse had been saturated it was slowly drained to field capacity. The drainable porosity was calculated from the volume of leachate drained, per unit total volume. If the waste was already at field capacity prior to saturation, the drainable porosity could also be calculated from the volume of water taken to saturate a unit volume of waste. The water content at field capacity was calculated from the total mass of water retained by the sample.

25. The hydraulic conductivity of the refuse at each vertical load was determined by carrying out a constant head flow test. Water from the header tanks was allowed to flow upward through the refuse, overflowing at the top of the column. The hydraulic gradient was determined by means of piezometers inserted through the ports in the side of the column. Different piezometers at the same horizon indicated the same hydraulic head, suggesting that flow was indeed vertical and that the distribution of flow over each cross-section was approximately uniform.

26. In general, the variation of hydraulic conductivity with depth within the cell was bilinear, with the hydraulic conductivity in the lower section being greater than that in the upper section. This is consistent with the reduction in the effective stress with depth arising from the effects of sidewall friction. In interpreting the data, the average hydraulic conductivity over the top and bottom sections of the cell was plotted separately against the average effective stress in each case.

27. The flow rate was measured using the electromagnetic flowmeters, except at low flow

rates when direct measurement of the (small) fall in water level in the header tanks with time was found to be more reliable.

28. The refuse was then drained, the applied stress increased and the cycle of operation and measurement repeated. The design and operation of the Pitsea compression cell is described in more detail by Beaven and Powrie⁹ and Beaven.⁶

Refuse classification

29. In this paper, the results from tests on one sample (designated DM3) of crude (i.e. unprocessed and undegraded) household waste obtained direct from the tipping face of a landfill are presented. Results of tests on other waste materials are reported by Beaven and Powrie⁹ and Beaven.⁶ Compression tests were undertaken after the refuse had been brought up to field capacity (at an applied load of 40 kPa) by saturation and subsequent drainage. The water content at the start of compression was approximately 101% (by dry mass).

30. Samples of the refuse were analysed at Warren Spring Laboratories (now AEA Technology), and categorized by the percentage of the total weight of individual components such as paper, plastics, textiles, etc. (Table 1).

31. Each sample of waste was in the compression cell for approximately six months during a test. It was considered unlikely that significant degradation would have occurred over this time period under the test conditions imposed, and visual inspection of the samples at the end of each test confirmed this. The main potential impact of degradation over this time-scale would be the effect of gas on the measured hydraulic conductivity, but there was no evidence of anything other than modest gas generation rates during the experiment.

Results

32. The calculation of the effective stress, transmitted through the waste by interparticle contact, at which each parameter was measured, is not as straightforward as it might at first appear.

33. First, the average vertical total stress in the waste is less than the applied pressure, owing to friction losses at the sidewalls. The average total stress has been taken as the total stress at the midpoint of the waste at the end of any compression stage, calculated using equation (3) with $\phi' = 40^\circ$ and $\delta = 30^\circ$ as already discussed. When the sample is free to drain and downward flow has ceased, it is assumed that the gauge pore water pressure is zero so that the average total and effective stresses are equal. The error bars in Figs 4 and 5 encompass the applied stress as the maximum possible

Table 1. Material classification of household waste tested (sample DM3)

Refuse component	Dry density of component: Mg/m ³	Saturated density of component: Mg/m ³	% of total mass
Paper/card	0.4*	1.2*	39.9
Plastic film	1.0*	1.0*	4.4
Dense plastics	1.1*	1.1*	6.4
Textiles	0.3*	0.6*	5.5
Misc. combustibles	1.0†	1.2†	11.8
Misc. non-combustibles	1.8*	2.0*	2.4
Glass	2.9*	2.9*	7.0
Putrescibles	1.0*	1.2†	13.3
Ferrous metals	6.0*	6.0*	3.2
Non-ferrous	6.0†	6.0†	1.2
Fines (< 10 mm)	1.8†	2.0†	4.9
Total	—	—	100.0

*From Landva and Clark.¹⁰

†Assumed value.

value and the transmitted stress calculated using equation (3) with $\phi' = \delta = 38^\circ$ as a minimum.

34. Second, during a hydraulic conductivity test, the introduction of a high pore water pressure at the base will result in reduced effective stresses throughout the sample. The average effective stress could be determined from the difference between the average total stress (calculated as previously described) and the average pore water pressure (as measured by the piezometers installed at various depths within the sample). However, Figs 4 and 5 relate to the maximum effective stress to which the sample had been subjected, as the rebound on introducing water at the base was very small.

Refuse density

35. Figure 4 shows the variation in the dry density, saturated density and density at field capacity of the refuse with vertical effective stress. The final dry density at an average vertical stress of 463 kPa was 0.72 Mg/m³. Wet densities in the range 0.62–0.67 Mg/m³ and 0.81–1.11 Mg/m³ were reported by Caterpillar¹¹ following compaction of crude domestic wastes in layers using Caterpillar 816B and 826 compaction plant.^{11,12} Assuming a water

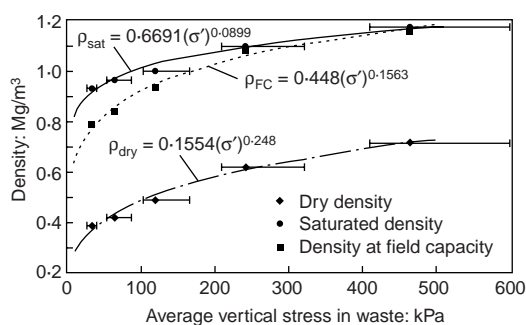


Fig. 4. Variation in refuse density with vertical effective stress

content of 30–40%, these ranges of wet density correspond to dry density ranges of 0.37–0.47 Mg/m³ and 0.49–0.78 Mg/m³ respectively. The implication is that, in terms of the waste density achieved, compaction at the tipping face can have a similar effect to the burial of the waste by several tens of metres of overburden. This should be taken into account in assessing the ease with which it may be possible to extract leachate from or control the movement of leachate within the waste in a landfill.

Drainable porosity and field capacity

36. The dry density, drainable porosity, and water content at field capacity at different vertical effective stresses are recorded in Table 2. The drainable porosity generally decreased (indicating an increasing degree of saturation) with increasing vertical effective stress σ'_v even under conditions of free downward drainage. At a vertical stress of 463 kPa the drainable porosity was less than 2%, suggesting that for practical purposes the waste may be treated as fully saturated at higher effective stresses. (This may not be the case for a gassing waste.)

37. When expressed as a ratio of mass of water to mass of dry solids, the water content at field capacity fell significantly with increasing vertical stress. However, the water content at field capacity expressed in volumetric terms does not change significantly with vertical stress.

Hydraulic conductivity

38. The saturated hydraulic conductivity at different applied stresses is shown in Table 2 and Fig. 5. Over the stress range investigated, the hydraulic conductivity fell by approximately three orders of magnitude.

Dry particle density and specific volume

39. The average density ρ_s of the waste particles is

$$\rho_s = \frac{m_s}{V_s} \tag{4}$$

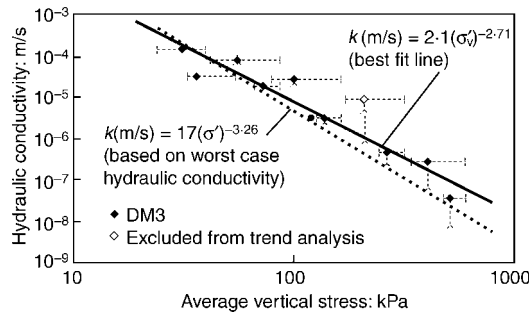


Fig. 5. Variation in saturated hydraulic conductivity with vertical effective stress for crude household waste

where m_s is the mass and V_s is the volume of (dry) solids. As

$$\rho_{dry} = \frac{m_s}{V_s + V_V}$$

$$\rho_s = v \cdot \rho_{dry} \tag{5}$$

40. The specific volume v of the waste at each stage of compression can be determined from the water content at field capacity expressed in volumetric terms (WC_{vol}) and the drainable porosity, n_e

$$v = \frac{V_s + V_V}{V_s} = \frac{1}{[1 - (WC_{vol} + n_e)]} \tag{6}$$

41. Table 3 indicates that the average particle density of the waste increases with applied stress. Given the deformable and crushable nature of the particles, this is not surprising. It is nonetheless an important finding, as it may cast doubt on the applicability to household waste of conventional soil mechanics theories of volume change such as compression and consolidation, in which it is normally assumed that the solid particles are incompressible and the particle density does not change significantly.

Implications for practice

Vertical drainage capacity of a landfill

42. The simplest way of flushing contaminants out of a landfill is to introduce uncontaminated liquid at the surface and allow it to percolate downward under gravity through the

Table 2. Dry density, drainable porosity and water content at field capacity, and saturated hydraulic conductivity of crude domestic waste at different vertical stresses

Applied stress: kPa	Average vertical stress: kPa	Dry density: Mg/m ³	Drainable porosity: %	WC _{dry} at field capacity: %	WC _{vol} at field capacity: %	Saturated hydraulic conductivity k : m/s
Initial	nd	0.32	nd	nd	nd	nd
40	34.1	0.39	14.7	101	40	1.5×10^{-4} to 3.4×10^{-5}
87	64.9	0.42	12.5	99	42	8.2×10^{-5} to 1.9×10^{-5}
165	120	0.49	6.5	91	45	2.8×10^{-5} to 3.1×10^{-6}
322	241	0.59	~2.0	76	45	8.9×10^{-6} to 4.4×10^{-7}
600	463	0.72	~1.5	62	44	2.7×10^{-7} to 3.7×10^{-8}

nd = not determined.

Table 3. Average particle density of household waste at different vertical stresses

Average vertical stress: kPa	Dry density, ρ_{dry} : Mg/m ³	Water content at FC, WC_{vol} : %	Drainable porosity, n_e : %	Volume of voids, V_v : %	Volume of solids, V_s : %	Specific volume, v	Average particle density, ρ_s : Mg/m ³
34	0.39	41.1	14.4	55.5	44.5	2.247	0.876
65	0.43	43.0	12.6	55.6	44.4	2.252	0.968
120	0.50	44.5	6.5	51.0	49.0	2.041	1.020
241	0.62	45.0	2.0	47.0	53.0	1.887	1.170
463	0.71	44.0	1.5	45.5	54.5	1.835	1.303

waste mass to be collected in a drainage blanket. The hydraulic head in the drainage blanket is controlled by pumping and could if necessary be maintained at or near zero. Examples of infiltration ponds being used to recirculate leachate through landfills in this way are reported by Townsend *et al.*¹³

43. In a landfill in which the hydraulic conductivity of the waste is uniform with depth, a uniform downward hydraulic gradient of unity would be established and the steady-state infiltration rate (in m³/s of liquid per m² surface area of the landfill) would be equal to the hydraulic conductivity of the waste. The results of the tests carried out in the Pitsea compression cell show that, in reality, the hydraulic conductivity of the refuse is likely to decrease with depth. In these circumstances in saturated steady-state flow, the downward hydraulic gradient is not uniform with depth, but increases as the hydraulic conductivity k decreases to give a volumetric flux q/A (i.e. the flow rate q per unit cross-sectional area A) that is constant with depth z ; according to Darcy's law

$$\frac{q}{A} = k \cdot \frac{\partial h}{\partial z} \quad (7)$$

where h is the hydraulic head. This type of behaviour is well-documented for soil deposits in which the hydraulic conductivity changes with depth.^{14,15}

44. For refuse, the situation is more complicated than for most soils, because in addition to the hydraulic conductivity k , the unit weight γ also varies significantly with vertical effective stress σ'_v . The vertical effective stress σ'_v depends in turn on the vertical total stress (which depends on the unit weight γ) and on the pore water pressure u (which depends on the head h and hence on the hydraulic conductivity k).

45. Figure 6 shows a layer of thickness δz whose upper surface is at a depth z below the surface of a landfill of overall depth D . The hydraulic head (measured above the base of the landfill) at depth z is h , and the hydraulic head at depth $z + \delta z$ is $h - \delta h$. Thus the hydraulic gradient at depth z is $\delta h/\delta z$.

46. The changes in vertical total stress $\delta \sigma_v$,

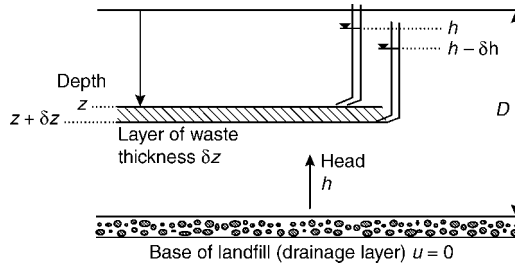


Fig. 6. Analysis of vertical infiltration through a landfill

pore water pressure δu and vertical effective stress $\delta \sigma'_v$ that take place over the depth increment δz are as follows

$$\delta \sigma_v = \rho_{sat} \cdot g \cdot \delta z \quad (8)$$

$$\delta u = \rho_w \cdot g \cdot (\delta z - \delta h) \quad (9)$$

$$\delta \sigma'_v = \delta \sigma_v - \delta u \quad (10)$$

while from Darcy's law

$$(q/A) = k \cdot i = k \cdot (\delta h/\delta z), \text{ or}$$

$$\delta h = (q/A) \cdot (1/k) \cdot \delta z \quad (11)$$

47. The saturated density ρ_{sat} and hydraulic conductivity k may be related to the vertical effective stress using the data given in Figs 4 and 5

$$\rho_{sat} (\text{Mg/m}^3) = 0.6691 \times (\sigma'_v)^{0.0899} \quad (12)$$

$$k (\text{m/s}) = 2.1 \times (\sigma'_v)^{-2.71} \quad (13)$$

where in both cases σ'_v is in kPa.

48. Distributions of vertical effective stress σ'_v and pore water pressure u with depth within a landfill, together with an infiltration rate q/A , that satisfy equations (8)–(13), subject to the conditions $\sigma_v = 40$ kPa (representing for example the effect of a cap approximately 2 m thick) and $u = 0$ at $z = 0$, and $u = 0$ at $z = D$ (representing a pumped basal drainage layer), can be calculated for a given value of D using a spreadsheet. These are shown for $D = 30$ m in Fig. 7. The relationships given in equations (12) and (13) assume that the waste has not been precompacted, or overconsolidated as a result of placement prior to saturation.

49. The large reduction in hydraulic conductivity over the bottom few metres of the landfill was a feature of all of the spreadsheet analyses, and became more pronounced as the

depth of the landfill was increased. The calculation shows that a very low hydraulic conductivity at the base of a landfill need not represent a significant barrier to vertical flow, because of the high vertical hydraulic gradients that will develop to compensate.

50. The effect of a greater leachate head in the basal drain is illustrated in Fig. 8. Although this results in a smaller effective stress and hence a higher hydraulic conductivity (assuming that there has been no precompaction or overconsolidation), this is more than offset by the reduced hydraulic gradient with the result that overall the flow rate is reduced. If the leachate head in the basal drain is increased in an attempt to promote upward flow, a vertical effective stress of zero is calculated at the base of the landfill when the head in the basal drain reaches 30.4 m, that is, only 0.4 m above the top of the waste. This does not necessarily rule out upward flushing (especially in situations where there is a large surcharge), but in Fig. 8 the maximum flow rate is for downward flow with the basal drain maintained at zero pore water pressure.

51. The infiltration rate calculated according to equations (8)–(13) is plotted as a function of landfill depth in Fig. 9, where it is compared with the maximum infiltration rate that prevents the build-up of leachate heads anywhere within the landfill. The latter infiltration rate has been calculated on the basis of a unit hydraulic gradient and the lowest hydraulic conductivity present in a vertical section. In the absence of any low permeability cover material, this will occur at the base of the site.

52. Both of the curves shown in Fig. 9 have been calculated on the basis of the relationship between hydraulic conductivity and stress derived for fully saturated wastes. In unsaturated waste, the hydraulic conductivity will be lower than that measured in saturated waste. The infiltration rates plotted in Fig. 9 should therefore be considered as absolute maxima.

53. The infiltration rate (in m/annum) required to flush contaminants from a landfill over a time-scale of 50 years is given approximately by the depth of the landfill in metres divided by 10.¹⁶ Fig. 9 shows that if the likely variation in hydraulic conductivity with depth is taken into account and if saturated conditions are allowed to develop in the landfill (but not necessarily in the basal drainage layer), much greater infiltration rates are calculated and the maximum depth of landfill for which a satisfactory flushing rate can apparently be achieved is substantially increased.

54. However, if the as-placed density is increased (reflecting, for example, the effects of compaction of the waste at the tipping face), the variation in hydraulic conductivity with depth and the overall infiltration rate are both reduced. The second of these is illustrated in

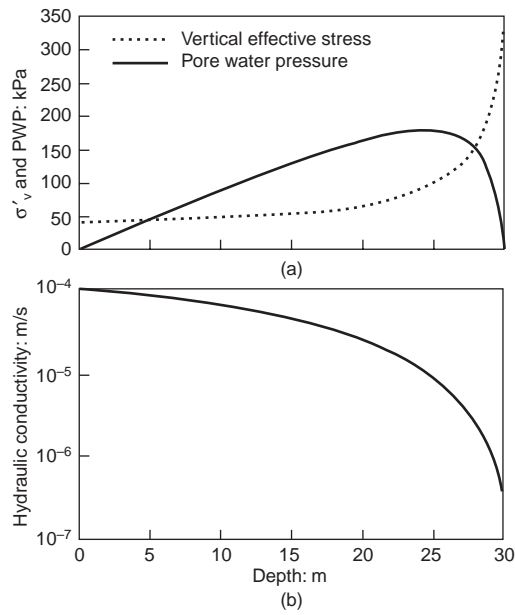


Fig. 7. Variation in: (a) vertical effective stress and pore water pressure; and (b) hydraulic conductivity with depth in a 30 m deep landfill with downward leachate flow

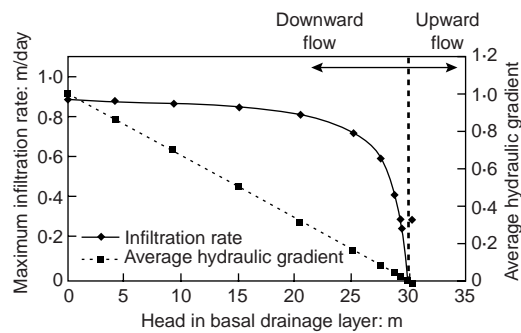


Fig. 8. Maximum infiltration rate against head in basal drainage layer of a 30 m deep landfill

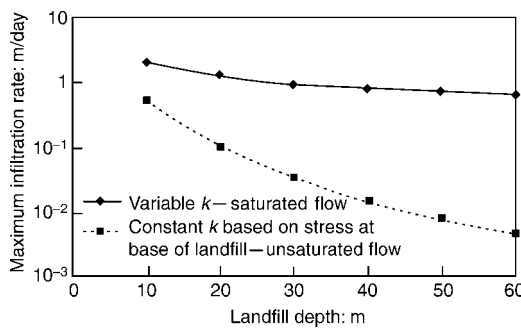


Fig. 9. Vertical infiltration rate against landfill depth

Fig. 10, where maximum infiltration rates have been plotted against precompacted waste densities based on the original water content of the waste DM3 as received ($WC_{dry} = 51.5\%$). Fig. 10(a) is based on the relationship $k = 2.1(\sigma')^{-2.71}$ (i.e. the best-fit relationship between hydraulic conductivity and vertical effective stress shown in Fig. 5), while Fig. 10(b) is based on $k = 17(\sigma')^{-3.26}$ (the worst-case relationship in Fig. 5). The flushing rate of $0.1 \times$ the landfill depth is also indicated, converted to units of m/day. Taking the best-case fit relationship between hydraulic conductivity and vertical effective stress, Fig. 10(a) suggests that it is only for well-compacted wastes that

this required flushing rate will not be achieved ($\rho_{wet} > 1.1 \text{ Mg/m}^3$ for sites between 0 and 30 m deep, and $\rho_{wet} > 1.0 \text{ Mg/m}^3$ for sites up to 60 m deep). For the worst-case fit of hydraulic conductivity to stress, precompaction densities must be less than 1.0 Mg/m^3 for sites less than 30 m deep, and less than 0.9 Mg/m^3 for sites up to 60 m deep.

55. In calculating the relationships shown in Fig. 10, the precompacted waste densities based on a constant water content ($WC_{dry} = 51.5\%$) have been converted to saturated waste densities (required for the calculation of stresses with depth) using the relationship between dry density and stress shown in Fig. 4. It has also been assumed that

- (a) the waste density does not increase due to relaxation of the waste above the level at which the as-placed density is in equilibrium with the vertical effective stress due to self-weight effects
- (b) below this level the relationship between density and vertical effective stress is as shown in Fig. 4
- (c) the landfill consists entirely of household waste and there are no layers of other materials which could impede or channel flow.

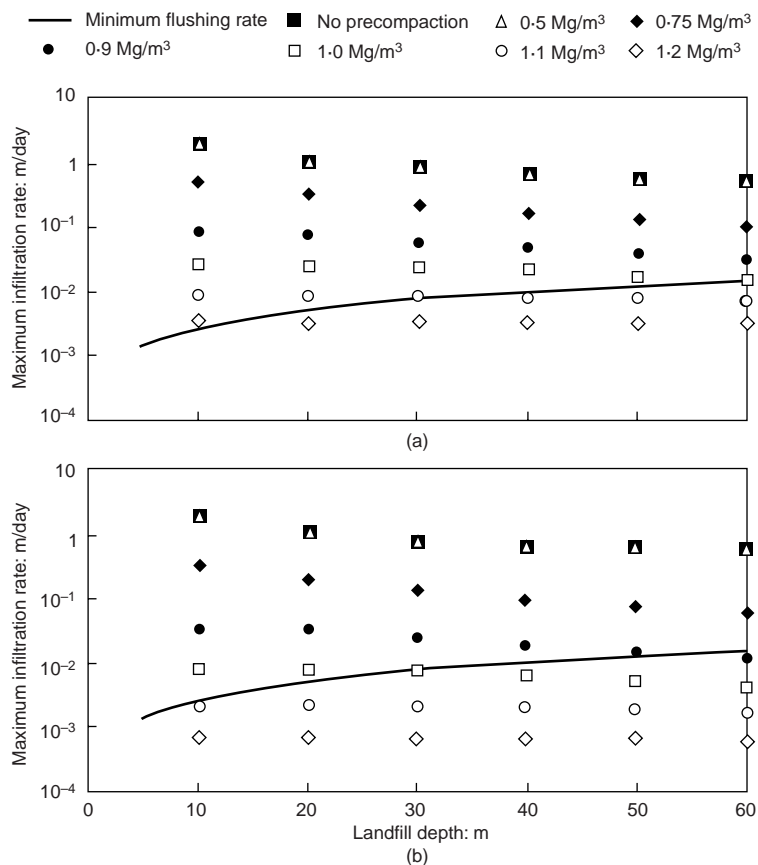
56. Owing to the possible presence of low permeability layers (e.g. daily cover), and the likely reduction in hydraulic conductivity that will occur as the waste degrades, the infiltration rates given in Fig. 10 probably err on the high side. Long-term design should probably be based on the properties of aged or degraded wastes, which might be expected to be of lower hydraulic conductivity than when fresh owing to particle size reduction and density increase, but the underlying principles would be the same.

Effect of pumping from vertical wells

57. One of the main potential pathways by which a landfill might pollute the environment is the leakage of leachate into the surrounding ground through the base and/or sides. In the case of a conventional landfill, such leakage can be prevented or at least minimized by maintaining the leachate level within a landfill below a certain limit. At old sites, landfill operators usually have no option but to seek to achieve this by pumping leachate from vertical wells, but generally with only limited success because yields from vertical wells in landfills are often very low.

58. The reasons for the apparent ineffectiveness of vertical leachate wells in waste are not certain, but may include any or all of the following

- (a) disturbance to the formation during drilling (e.g. milling and/or smearing of the waste)



- (b) poor filter pack and wellscreen design
- (c) clogging of the filter pack or wellscreen
- (d) interference between gas and liquid phases within the waste
- (e) a failure to develop the well after installation
- (f) the generally low hydraulic conductivity of wastes
- (g) large drawdowns, which may reduce the thickness of waste available for flow
- (h) a reduction in waste hydraulic conductivity near the well, due to increased effective stresses.

59. An initial appreciation of the impact of the last three of these may be obtained by substituting equation (13) into Darcy's law in the standard Dupuit analyses⁴ for horizontal radial flow to wells in ideal confined and unconfined aquifers (Fig. 11; the full analyses are given in Appendix 2). The resulting relationships between well drawdown and well yield are shown in Fig. 12. For comparison, the relationships obtained for materials in which the hydraulic conductivity does not change as the drawdown is increased are also shown.

60. The analyses take no account of well losses that will occur in close proximity to the well, such as head losses from flow through the well screen, a possible limiting hydraulic gradient in the vicinity of the well¹⁷ and seepage face effects. Also, the effects of lower permeability layers and waste degradation have not

Fig. 10. Infiltration rate for:
(a) $k = 2.1(\sigma')^{-2.71}$;
and
(b) $k = 17(\sigma')^{-3.26}$
against landfill depth for various precompacted waste densities. (All waste densities at a water content (WC_{dry}) of 51.5% (assumed WC of waste as deposited))

been considered. At a given drawdown, the actual yield of a well in the field must therefore be expected to be less than indicated in Fig. 12.

61. In the case of the confined aquifer (Fig. 12(a)), the well yield increases with drawdown. However, the specific capacity (i.e. the flow rate per unit drawdown) decreases with increasing drawdown. The calculated well yields are probably rather greater than would be achieved in practice, as the effects of precompaction on waste density and hydraulic conductivity were not modelled in the analysis.

62. The unconfined aquifer analysis (Fig. 12(b)) is more representative of field conditions at many landfills. At low drawdowns, the flow rates and specific capacities are higher than in the confined aquifer analysis because the initial saturated thicknesses (D) is twice as great. The flow rate again increases with drawdown, but in this case there is little increase in flow rate for increases in drawdown in excess of about 50% of the initial saturated depth.

63. In reality, the distance of influence of the well might be expected to increase with increasing drawdown. The effect of this has not been taken into account in the analyses presented in Fig. 12, in which it has been assumed that the distance of influence is constant. The effect of increasing the distance of influence with drawdown would be to reduce further the specific yield at large drawdowns, which reinforces the point already made concerning the effect of drawdown on well performance.

64. In both the well and the vertical infiltration analyses, a reduction in the leachate head in the well or the basal drain increases the hydraulic gradient. It also increases effective stresses and reduces the hydraulic conductivity of the waste. In the vertical infiltration analysis, the increase in the hydraulic gradient is the dominant effect and the overall flow rate increases. In the confined aquifer well analysis, the increase in hydraulic gradient dominates but to a lesser extent owing to the reduction in flow area as the well is approached. In the case of the unconfined aquifer well analysis, the additional reduction in flow area resulting from the decrease in saturated thickness as the well is approached causes the decrease in permeability to dominate, and the flow rate may start to decrease with increasing drawdown.

65. In addition, long-term flow rates should ideally be assessed on the basis of the properties of aged or degraded wastes, which might be expected to be of somewhat lower hydraulic conductivity than when fresh, owing to the effects of particle size reduction and an increased bulk density. This is an area of continuing research.

Conclusions

66. The quantification of the hydraulic properties and geotechnical behaviour of land-

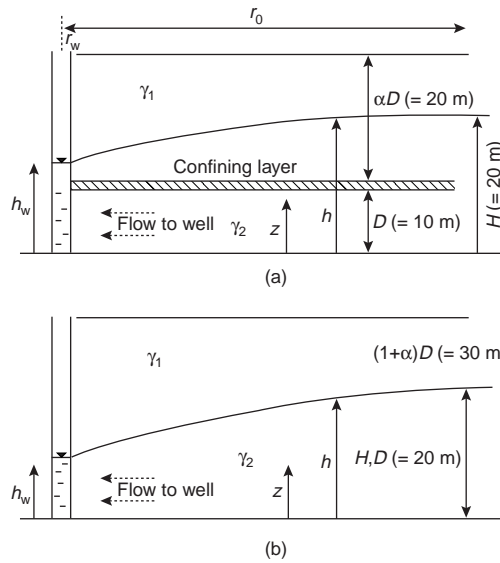


Fig. 11. Ideal: (a) confined; and (b) unconfined aquifer analyses. (In both analyses $\ln(r_o/r_w) = 8$ and the unit weight of saturated and unsaturated waste = 11 kN/m^3)

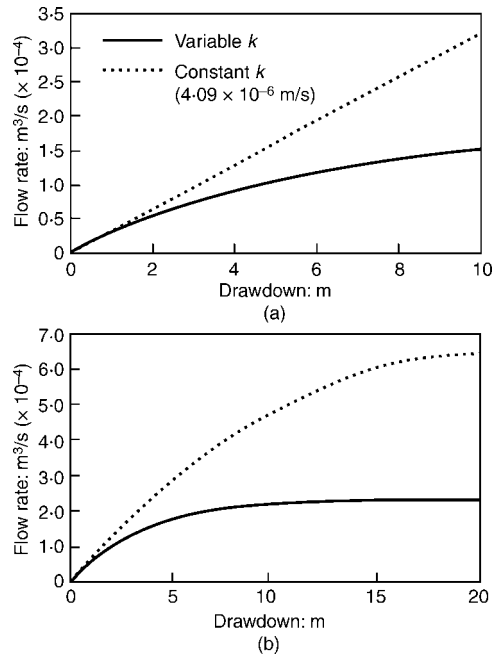


Fig. 12. Relationship between discharge rate and drawdown for approximate ideal: (a) confined; (b) unconfined aquifer analyses in which the hydraulic conductivity varies with drawdown according to equation (13)

filled waste is complex. This is partly because of the variable, deformable and degradable nature of its constituents, and partly because the material is often in an unsaturated state with gaseous, liquid and solid phases present. The field capacity of the refuse, which is defined as the equilibrium water content (mass of water to mass of dry solids) at a certain vertical stress under conditions of free vertical drainage, represents a useful reference state.

67. Although the concepts of conventional soil mechanics offer a convenient framework within which the behaviour of wastes can be described and understood, the applicability of certain standard theories may need to be reconsidered in the light of the significant increase in particle density that occurs with increasing stress.

68. A compression test on a non-degraded unsaturated waste at field capacity has demonstrated the variability of the actual and dry density and drainable porosity (drainable void volume) with vertical stress. For example, the drainable porosity of domestic refuse fell from 14.7% to less than 2% at an average vertical stress of approximately 480 kPa. The test has also shown that the hydraulic conductivity of saturated domestic waste, such as would be expected to be found near the base of a landfill, could fall by over three orders of magnitude to $\sim 10^{-8}$ m/s between placement and burial to a depth of 60 m due to the effects of compression alone.

69. The variation with vertical stress (and hence with depth in a landfill) of the hydraulic properties of waste has significant implications for landfill management in general, and the design of leachate control systems in particular. This has been illustrated by means of two example calculations using simplified analytical models. In particular, the following points are highlighted.

- (a) The variation in hydraulic conductivity with effective stress and hence with depth within the landfill must be taken into account in the calculation of vertical infiltration rates. Much higher infiltration rates can be achieved in sites where leachate heads within the body of the site are allowed to develop than in unsaturated sites.
- (b) The reduction in hydraulic conductivity with increasing effective stress will adversely affect the performance of a vertical leachate extraction well at large drawdowns. The specific yield (i.e. flow rate per unit drawdown) must be expected to decrease as the drawdown in the well is increased, and there may well be no significant increase in flow rate when the drawdown in the well is increased beyond a certain value.

70. The properties of non-degraded domestic refuse could be used in the design of leachate collection and recirculation systems which may be required in future to achieve more rapid landfill stabilization. However, the effects of landfill processes that alter the bulk properties of the material must also be addressed. In particular, the use of low hydraulic conductivity daily cover and modern landfill compaction techniques may impede the free flow of leachate within a landfill necessary to achieve stabilization. In addition, long-term flow rates should ideally be assessed on the basis of the properties of aged or degraded wastes, which might be expected to be of lower hydraulic conductivity than when fresh, owing to particle size reduction and density increase; this is an area of further research.

Acknowledgements

71. The research presented in this paper was funded by the Waste Technical Division of the UK Department of the Environment, Cleanaway Ltd and the Engineering and Physical Sciences Research Council. The views expressed in this paper are those of the authors and do not necessarily represent those of any of these organizations.

Appendix 1. Calculation of the effect of sidewall friction on the transmission of vertical stress in the compression cell⁶

72. The forces and stresses acting on a thin layer of waste at depth z within the compression cell were shown in Fig. 2.

73. The difference $A.\delta\sigma'_v$ between the total vertical force applied to the top of a layer of vertical thickness δz and the total vertical force transmitted at the bottom of the layer is equal to the weight of refuse within the layer minus the frictional force exerted by the cell on the perimeter of the layer.

74. The shear stress τ is equal to the product of the normal effective stress and the tangent of the angle of friction (δ) between the refuse and wall of the compression cell. The frictional force F is

$$F = \sigma'_h \cdot \tan(\delta) \pi \cdot d \cdot \delta z$$

Vertical equilibrium of the layer requires that

$$A.\delta\sigma'_v = \gamma.A.\delta z - \pi.d.\delta z(\sigma'_h \tan \delta)$$

Rearranging and setting

$$A = \frac{\pi d^2}{4}$$

$$\delta z(\gamma d - 4\sigma'_h \tan \delta) = d\delta\sigma'_v$$

or

$$\frac{d\sigma'_v}{dz} = \gamma - \frac{4\sigma'_h \tan \delta}{d} \quad (14)$$

75. The horizontal effective stress may be related to vertical effective stress⁵ by

$$\sigma'_h = (1 - \sin \phi') \sigma'_v \quad (15)$$

$$\frac{d\sigma'_v}{dz} = \gamma - \left[\frac{4(1 - \sin \phi') \tan \delta}{d} \right] \cdot \sigma'_v \quad (16)$$

76. Assuming that ϕ' , δ and γ remain constant and are independent of depth z within the cell, let

$$B = \left[\frac{4(1 - \sin \phi') \tan \delta}{d} \right] \quad (17)$$

77. Substituting B into equation (16) gives

$$\frac{d\sigma'_v}{dz} = \gamma - B.\sigma'_v \quad (18)$$

78. Integrating with respect to vertical effective stress and depth gives

$$\int_p^{\sigma'_v} \frac{d\sigma'_v}{\gamma - B.\sigma'_v} = \int_0^z dz \quad (19)$$

where \mathbf{P} is the applied surface load, or

$$\sigma'_v = \frac{\gamma}{B}(1 - e^{-Bz}) + \mathbf{P}.e^{-Bz} \quad (20)$$

Appendix 2. Approximate analysis of axisymmetric horizontal flow to wells in confined and unconfined aquifers with a stress-dependent hydraulic conductivity

Confined aquifer

79. The geometry and terms for the confined aquifer analysis are defined in Fig. 11(a). At a general depth z , the vertical total stress σ_v is

$$\sigma_v = \gamma_1.(1 + \alpha).D - h] + \gamma_2.(h - z) \quad (21)$$

80. The pore water pressure \mathbf{u} is

$$\mathbf{u} = \gamma_w.(h - z) \quad (22)$$

Hence

$$\begin{aligned} \sigma'_v &= \sigma_v - \mathbf{u} = \gamma_1.(1 + \alpha).D - h] \\ &+ \gamma_2.(h - z) - \gamma_w.(h - z) \\ \Rightarrow \sigma'_v &= \gamma_1.(1 + \alpha).D - (\gamma_1 - \gamma'_2).h \\ &- (\gamma_2 - \gamma_w).z \end{aligned}$$

$$\text{or } \sigma'_v = C - E.h - \gamma'_2.z \quad (23)$$

where $C = \gamma_1.(1 + \alpha).D$, $E = (\gamma_1 - \gamma'_2)$ and $\gamma'_2 = [\gamma_2 - \gamma_w]$.

81. Assuming horizontal flow, the flow rate δq at radius r through a horizon of thickness δz at an elevation z is, by Darcy's law

$$\delta q = 2.\pi.r.\delta z.k.\left(\frac{\partial h}{\partial r}\right) \quad (24)$$

where k is the hydraulic conductivity, which varies with vertical effective stress according to equation (25),

$$k = A.(\sigma'_v)^{-B} \quad (25)$$

and A and B are experimentally determined constants.

82. Substituting equation (23) into equation (25) and the result into equation (24) yields

$$\delta q = 2.\pi.A.r.(C - E.h - \gamma'_2.z)^{-B}.\left(\frac{\partial h}{\partial r}\right).\delta z \quad (26)$$

83. Equation (26) can be integrated with respect to q and z to determine the total flow rate through a cylinder of radius r and height D

$$\begin{aligned} \int_0^q dq &= 2.\pi.A.r.\frac{\partial h}{\partial r} \int_0^h (C - E.h - \gamma'_2.z)^{-B} dz, \text{ or} \\ q &= 2.\pi.r.\frac{\partial h}{\partial r}.\frac{A}{\gamma'_2.(B-1)}.\{(C - Eh - \gamma'_2 D)^{-(B-1)} \\ &- (C - Eh)^{-(B-1)}\} \end{aligned} \quad (27)$$

84. Integrating again with respect to h and r , between limits of $h = H$ at the radius of

influence $r = r_o$ and $h = h_w$ at $r = r_w$ just outside the well, yields

$$\begin{aligned} q &= \frac{2.\pi.A}{E.\gamma'_2.(B-1)(B-2).\ln\left(\frac{r_o}{r_w}\right)} \\ &\times \{C - Eh - \gamma'_2 D\}^{-(B-2)} - (C - Eh)^{-(B-2)} \\ &- (C - Eh_w - \gamma'_2 D)^{-(B-2)} + (C - Eh_w)^{-(B-2)} \} \end{aligned} \quad (28)$$

Unconfined aquifer

85. The geometry and terms for the unconfined aquifer analysis are defined in Fig. 11(b). At a general depth z , the vertical total stress σ_v is

$$\sigma_v = \gamma_1.(1 + \alpha).H - h] + \gamma_2.(h - z) \quad (29)$$

The pore water pressure \mathbf{u} is

$$\mathbf{u} = \gamma_w.(h - z) \quad (30)$$

Hence

$$\sigma'_v = \sigma_v - \mathbf{u} = \gamma_1.(1 + \alpha).H + \gamma'_2.(h - z) - \gamma_1.h$$

or

$$\sigma'_v = E - C.h - \gamma'_2.z \quad (31)$$

where $C = \gamma_1.(1 + \alpha).H$, $E = (\gamma_1 - \gamma'_2)$ and $\gamma'_2 = [\gamma_2 - \gamma_w]$.

86. Assuming horizontal flow, the flow rate δq at radius r through a horizon of thickness δz at an elevation z is, by Darcy's law

$$\delta q = 2.\pi.r.\delta z.k.\left(\frac{\partial h}{\partial r}\right) \quad (32)$$

where the hydraulic conductivity k again varies with vertical effective stress according to equation (25).

87. Substituting equation (31) into equation (25) and the result into equation (32)

$$\delta q = 2.\pi.A.r.[C - E.h - \gamma'_2.z]^{-B}.\left(\frac{\partial h}{\partial r}\right).\delta z \quad (33)$$

88. Integrating equation (33) with respect to q and z to determine the total flow rate through a cylinder of radius r and height h

$$\begin{aligned} \int_0^q dq &= 2.\pi.A.r.\frac{\partial h}{\partial r} \int_0^h [C - E.h - \gamma'_2 z]^{-B} dz, \text{ or} \\ q &= 2.\pi.r.\frac{\partial h}{\partial r}.\frac{A}{\gamma'_2.(B-1)} \\ &\times \{[C - (E + \gamma'_2)h]^{-(B-1)} - (C - Eh)^{-(B-1)}\} \end{aligned} \quad (34)$$

89. Integrating again with respect to h and r , between limits $h = H$ at the radius of influence $r = r_o$, and $h = h_w$ at $r = r_w$ just

outside the well, and noting that $E + \gamma'_2 = \gamma_1$, yields

$$q = \frac{2\pi A}{\gamma'_2(B-1)(B-2) \cdot \ln\left(\frac{r_o}{r_w}\right)} \times \left\{ \frac{(C - \gamma_1 H)^{-(B-2)} - (C - \gamma_1 h_w)^{-(B-2)}}{\gamma_1} - \frac{(C - E.H)^{-(B-2)} - (C - E.h_w)^{-(B-2)}}{E} \right\} \quad (35)$$

References

- HARRIS R. C., KNOX K. and WALKER N. A strategy for the development of sustainable landfill design. *Proceedings of the Institute of Waste Management*, 1994, Jan., pp. 26–29.
- DEPARTMENT OF THE ENVIRONMENT. *Landfill Design, Construction and Operational Practice*. HMSO, London, 1995, DOE waste management paper 26B.
- DEPARTMENT OF THE ENVIRONMENT. *Making Waste Work—A Strategy for Sustainable Waste Management in England and Wales*. HMSO, London, 1995.
- POWRIE W. *Soil Mechanics: Concepts and Applications*. E & F N Spon, London, 1997.
- JAKY J. The coefficient of earth pressure at rest. *Journal of the Hungarian Society of Architects and Civil Engineers*, 1994, 355–358.
- BEAVEN R. P. *The Hydrogeological and Geotechnical Properties of Waste in Relation to Sustainable Landfilling*. PhD dissertation, University of London (Queen Mary and Westfield College), 1999.
- JESSBERGER H. L. and KOCKEL R. Mechanical properties of waste materials. *XV Ciclo di Conferenze di Geotecnica di Torino*, 19–22 Nov. 1991.
- POLL A. J. *Sampling and Analysis of Domestic Refuse—A Review of Procedures at Warren Spring Laboratory*. Warren Spring Laboratory, Stevenage, 1988, technical report LR667 (MR)M.
- BEAVEN R. P. and POWRIE W. Determination of the hydrogeological and geotechnical properties of refuse using a large compression cell. *Proceedings of the 5th International Conference on Landfills, Sardinia 95* (Christensen T. H., Cossu R. and Stegmann R. (eds)). CISA Environmental Sanitary Engineering Centre, Cagliari, 1995, vol. 2, 745–760.
- LANDVA A. O. and CLARK J. I. Geotechnics of waste fill. In *Geotechnics of Waste Fills—Theory and Practice*, Baltimore (Landva A. and Knowles G. D. (eds)). ASTM STP 1070, 1990.
- CATERPILLAR. *Cat® 816B and 826C Compaction Study vs Hanomag CD 280, Bomag 601 RB*. Caterpillar Product Information Performance Report, January 1995.
- BEAVEN R. P. and POWRIE W. Determination of the hydrogeological and geotechnical properties of refuse in relation to sustainable landfilling. *Proceedings of the 19th International Madison Waste Conference*, University of Wisconsin–Madison, Wisconsin, 1996, 435–454.
- TOWNSEND T. G., MILLER W. L. and EARLE J. F. K. Leachate recycle infiltration ponds. *Journal of Environmental Engineering*, 1995, **121**, No. 6, 465–471.
- VAUGHAN P. R. Thirty-fourth Rankine Lecture: Assumption, prediction and reality in geotechnical engineering. *Géotechnique*, 1994, **44**, No. 4, 573–609.
- BROMHEAD E. N. Interpretation of pore water pressure profiles in underdrained strata. In *Groundwater Problems in Urban Areas* (Wilkinson W. B. (ed.)). Thomas Telford, London, 1994, pp. 149–158.
- WALKER A. N., BEAVEN R. P. and POWRIE W. P. Overcoming problems in the development of a high rate flushing bioreactor. *Proceedings of the 6th International Sardinia Landfill Symposium, S. Margherita di Pula*, Cagliari, Italy, October 1997, **1**, 397–408.
- PREENE M. and POWRIE W. Steady state performance of construction dewatering systems in fine soils. *Géotechnique*, 1993, **43**, No. 2, 191–205.

Please email, fax or post your discussion contributions to the Secretary:
email: Wilson_1@ice.org.uk; fax: 0171 799 1325; or post to Lesley Wilson,
Journals Department, Institution of Civil Engineers, 1–7 Great George Street,
London SW1P 3AA.